

Decretion disc size in Be/X-ray binaries depends upon the disc aspect ratio

Rebecca G. Martin^{1,2*} , Stephen H. Lubow³ , Philip J. Armitage^{4,5}  and Daniel J. Price⁶ 

¹Nevada Center for Astrophysics, University of Nevada, Las Vegas, 4505 South Maryland Parkway, Las Vegas, NV 89154, USA

²Department of Physics and Astronomy, University of Nevada, Las Vegas, 4505 South Maryland Parkway, Las Vegas, NV 89154, USA

³Space Telescope Science Institute, 3700 San Martin Drive, Baltimore, MD 21218, USA

⁴Center for Computational Astrophysics, Flatiron Institute, 162 Fifth Avenue, New York, NY 10010, USA

⁵Department of Physics and Astronomy, Stony Brook University, Stony Brook, NY 11794, USA

⁶School of Physics and Astronomy, Monash University, Vic. 3800, Australia

Accepted XXX. Received YYY; in original form ZZZ

ABSTRACT

With three-dimensional hydrodynamical simulations we show that the size of the decretion disc and the structure of the accretion flow onto the neutron star in a Be/X-ray binary strongly depends upon the disc aspect ratio, H/R . We simulate a Be star disc that is coplanar to the orbit of a circularly or moderately eccentric neutron star companion, thereby maximising the effects of tidal truncation. For low disc aspect ratio, $H/R \lesssim 0.1$, the disc is efficiently tidally truncated by the neutron star. Most material that escapes the Roche lobe of the Be star is accreted by the neutron star through tidal streams. For larger disc aspect ratio, the outflow rate through the Be star disc is higher, tidal truncation becomes inefficient, the disc fills the Roche lobe and extends to the orbit of the companion. Some material escapes the binary as a gas stream that begins near the L2 point. While the accretion rate onto the neutron star is higher, the fraction of the outflow that is accreted by the neutron star is smaller. Low density Be star discs are expected to be approximately isothermal, such that H/R increases with radius. Tidal truncation is therefore weaker for larger separation binaries, and lower mass primaries.

Key words: accretion, accretion discs - binaries: general – hydrodynamics - stars: emission-line, Be

1 INTRODUCTION

A Be/X-ray binary typically consists of a Be star with a neutron star companion (e.g. [Negueruela et al. 1998](#); [Coe et al. 2005](#); [Liu et al. 2005](#); [Reig 2011](#); [Haberl & Sturm 2016](#)). The Be star is rapidly rotating ([Slettebak 1982](#); [Porter 1996](#)) and material that is ejected from the Be star equator forms a decretion disc ([Pringle 1991](#); [Lee et al. 1991](#); [Carciofi 2011](#)). The outer radial extent of a Be star decretion disc may be limited by the tidal forces from the neutron star. If the disc is geometrically thin, then the outer edge of the disc occurs at the radius where tidal and viscous forces balance ([Papaloizou & Pringle 1977](#); [Artymowicz & Lubow 1994](#); [Okazaki et al. 2002](#); [Martin & Lubow 2011](#)). However, for circumplanetary discs with moderately large disc aspect ratio it has recently been shown that the effects of tidal truncation may be weak ([Martin et al. 2023](#)). Therefore the disc aspect ratio is an important parameter that can determine the size of disc.

Radiative equilibrium calculations for Be star discs suggest that heating by photoionization and collisional excitation is balanced by cooling from recombination and collisional de-excitation (e.g. [Sigut et al. 2009](#)). The predicted outer disc temperature is approximately isothermal, with $T \simeq 1 - 1.6 \times 10^4$ K, and the aspect ratio H/R increases with radius (e.g. [Carciofi et al. 2006](#); [Carciofi & Bjorkman 2006](#); [Rubio et al. 2023](#); [Suffak et al. 2023](#)). Observationally, the disc aspect ratio for Be star discs can be measured or constrained in several different ways ([Porter & Rivinius 2003](#); [Rivinius et al. 2013](#)).

By combining interferometry with polarimetry, an upper limit for ζ -Tau was found to be $H/R = 0.36$ (opening half angle of 20°) ([Quirrenbach et al. 1997](#)). Polarization can measure the inner parts of the disc, and ζ -Tau was found to have an aspect ratio of $H/R = 0.04$ (half-opening angle of 2.5°) ([Wood et al. 1997](#); [Carciofi et al. 2009](#)). Be star discs are thought to be flared, meaning that H/R increases with radius ([Hanuschik 1996](#)). In this case, systems with a larger binary orbital period may have a larger disc aspect ratio in the outer parts of the disc. Assuming a random distribution of the Be star disc inclination on the sky, statistics of shell stars suggest that the aspect ratio could be $H/R = 0.09$ (opening half-angle of 5°) ([Porter 1996](#)) or $H/R = 0.23$ (half-opening angle of 13°) ([Hanuschik 1996](#)). In general, these discs could have aspect ratios at least in the outer parts of the disc that are large enough to lead to a weakened tidal torque.

While observing the outer radius of a Be star disc is currently challenging (e.g. [Rivinius et al. 2013](#)), understanding the sizes of these discs has significant implications for observations of X-ray outbursts that occur when material is transferred to the neutron star. Be/X-ray binary star systems display two different types of outburst when material falls onto the neutron star. Type I outbursts occur each binary orbital period while Type II outbursts are brighter and occur less frequently ([Stella et al. 1986](#); [Negueruela et al. 1998, 2001](#); [Okazaki & Negueruela 2001](#); [Moritani et al. 2013](#); [Okazaki et al. 2013](#)). Type I outbursts may be driven by either an eccentric binary orbit, or an eccentric disc ([Franchini & Martin 2019](#)). Type II outbursts may be driven by a highly misaligned disc that undergoes ZKL ([von Zeipel 1910](#); [Kozai 1962](#); [Lidov 1962](#)) oscillations ([Martin et al. 2014a,b](#); [Fu et al. 2015](#)).

* E-mail: rebecca.martin@unlv.edu

Tidal truncation of Be star discs has been explored extensively in theoretical works (e.g. Okazaki & Negueruela 2001; Okazaki et al. 2002; Panoglou et al. 2016; Cyr et al. 2017; Suffak et al. 2022), however, the effect of a large disc aspect ratio has not been examined. In this work we determine the disc aspect ratio required for tidal truncation of Be star disc in a binary with a neutron star. We consider an idealized model of a Be star with a spin vector that is parallel to the binary angular momentum vector such that the Be star disc is coplanar to the binary orbit. This coplanar configuration sets an upper limit to the strength of the tidal torque (Lubow et al. 2015; Miranda & Lai 2015). The disc is constantly fed gas at a particular injection radius until a steady state (or quasi-steady state in the case of an eccentric orbit binary) disc is reached around the Be star. Section 2 describes the parameters for the Be/X-ray binary. Section 3 presents the results of 3D simulations of the Be star disc flow in which we show that the disc aspect ratio plays a key role in determining the amount of tidal truncation and the size of acretion disc in a Be/X-ray binary. Section 4 contains the conclusions.

2 BE/X-RAY BINARY PARAMETERS

We model a Be/X-ray binary with parameters motivated by those of 4U 0115+63 (e.g. Campana 1996; Negueruela et al. 1997). The Be star has a mass of $M_1 = 18 M_\odot$ and a radius of $R_1 = 8 R_\odot$. The companion neutron star has mass $M_2 = 1.4 M_\odot$ and is in an orbit with semi-major axis of $a_b = 95 R_\odot$. For this binary mass ratio, the Roche lobe radius of the Be star is $0.6 a_b = 56.8 R_\odot$ (Eggleton 1983). The binary orbit is either circular ($e_b = 0$) or mildly eccentric ($e_b = 0.34$). For the eccentric orbit simulations, the binary begins at apastron. The disc around the Be star is coplanar to the binary orbit so that it can reach a steady state disc structure. If the disc was inclined to the binary orbit, then it must undergo nodal precession (e.g. Papaloizou & Terquem 1995; Bate et al. 2000; Lubow & Ogilvie 2000) and finding a steady state is more complex. The tidal torque on a misaligned disc decreases with tilt above the orbital plane (Lubow et al. 2015; Miranda & Lai 2015). Therefore the tidal truncation radius found in this work is a lower limit. A misaligned disc may be larger and have a more significant outflow of material (Cyr et al. 2017).

Initially there is no gas in the simulation. Material is injected into the disc close to the Be star at a constant rate of $\dot{M}_{\text{inj}} = 10^{-10} M_\odot \text{ yr}^{-1}$ at a radius of $R_{\text{inj}} = 10 R_\odot$. The injection radius is chosen to be far from the stellar surface in order to increase the resolution of the simulations. If the injection radius is very close to the star, then an unphysically large fraction of the material falls immediately back onto the Be star (Nixon & Pringle 2020). This assumption changes the structure of the inner parts of the disc (Rímulo et al. 2018). However, in this work, we focus on the tidal truncation and therefore we are interested in the structure of the outer parts of the disc.

In the absence of the tidal field, it is possible to find steady state disc solutions assuming that the viscous torque is zero at both the inner edge of the disc, $R = R_{\text{in}}$, and the outer edge of the disc, $R = R_{\text{out}}$. In this case, the accretion rate onto the star is given by

$$\frac{\dot{M}_1}{\dot{M}_{\text{inj}}} = \frac{\sqrt{R_{\text{out}}} - \sqrt{R_{\text{inj}}}}{\sqrt{R_{\text{out}}} + \sqrt{R_{\text{inj}}}} \quad (1)$$

(Martin et al. 2023). Note that this estimate assumes Keplerian rotation in the disc and does not include any dependence on the disc

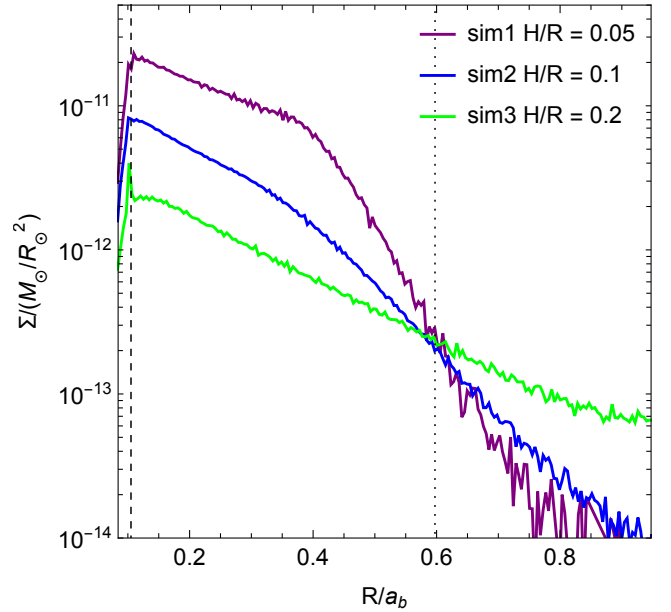


Figure 1. Azimuthally averaged steady state disc surface density profile at time $t = 50 P_{\text{orb}}$ for simulations with a circular orbit binary with $M_1 = 18 M_\odot$, $M_2 = 1.4 M_\odot$ and semi-major axis of $a_b = 95 R_\odot$. The disc has viscosity parameter $\alpha \approx 0.1$ and different disc aspect ratios, $H/R = 0.05$ (sim1), $H/R = 0.1$ (sim2) and $H/R = 0.2$ (sim3). The vertical dashed line shows the injection radius. The vertical dotted line shows the Roche lobe radius.

aspect ratio, H/R . The accretion outflow rate is given by

$$\frac{\dot{M}_{\text{dec}}}{\dot{M}_{\text{inj}}} = \left(1 - \frac{\dot{M}_1}{\dot{M}_{\text{inj}}} \right). \quad (2)$$

As the material leaves the Roche lobe of the Be star, it is accreted onto the neutron star at a rate \dot{M}_2 and ejected from the binary at a rate \dot{M}_{ej} . Therefore we can write

$$\dot{M}_{\text{dec}} = \dot{M}_2 + \dot{M}_{\text{ej}}. \quad (3)$$

However, in the analytical model we cannot distinguish between these two rates on the right hand side.

For our typical parameters with a circular orbit binary, we take $R_{\text{in}} = 8 R_\odot$, and $R_{\text{out}} = 60 R_\odot$ (this assumes that the disc is tidally truncated at this radius). For these parameters with equation (1) we have $\dot{M}_1/\dot{M}_{\text{inj}} = 0.93$ for $R_{\text{inj}} = 10 R_\odot$. Note that these estimates do not take into account the disc aspect ratio.

3 SPH SIMULATIONS

In order to include the effects of a tidal field from the companion neutron star and the effects of pressure, we must perform 3D hydrodynamical simulations. We use the smoothed particle hydrodynamics (SPH Monaghan 1992; Price 2012) code PHANTOM (Lodato & Price 2010; Price & Federrath 2010; Price et al. 2018). This has been well tested for tidal truncation of discs in binary star systems (e.g. Franchini & Martin 2019; Franchini et al. 2019; Heath & Nixon 2020; Hirsh et al. 2020). We note that our simulations are scaled to the injection accretion rate since we do not include disc self-gravity. The accretion rates in the steady state all scale with the mass injection rate.

The disc has a constant disc aspect ratio, H/R , with radius so

Name	H/R	α_{AV}	e_b	M_1	M_2	M_{part}/M_s	N_{steady}	$\langle h \rangle / H$	α	$\dot{M}_1/\dot{M}_{\text{inj}}$	$\dot{M}_2/\dot{M}_{\text{inj}}$	$\dot{M}_{\text{ej}}/\dot{M}_{\text{inj}}$
sim1	0.05	1.1	0.0	18	1.4	1×10^{-12}	76,000	0.74	0.08	0.978	0.019	0.003
sim2	0.1	2.9	0.0	18	1.4	1×10^{-13}	200,000	0.36	0.10	0.959	0.038	0.003
sim3	0.2	3.3	0.0	18	1.4	1×10^{-13}	95,000	0.30	0.10	0.932	0.048	0.019
sim4	0.1	0.29	0.0	18	1.4	2×10^{-13}	175,000	0.37	0.010	0.986	0.014	0.000
sim5	0.2	0.33	0.0	18	1.4	1×10^{-13}	115,000	0.28	0.009	0.972	0.019	0.009
sim6	0.1	2.9	0.34	18	1.4	1×10^{-13}	164,000	0.39	0.11	0.950	0.048	0.002
sim7	0.2	3.3	0.34	18	1.4	1×10^{-13}	92,000	0.31	0.10	0.931	0.048	0.021
sim8	0.1	2.9	0.0	10	1.4	1×10^{-13}	266,000	0.32	0.09	0.966	0.034	0.000

Table 1. The first seven columns describe the simulation input parameters: (left to right) the simulation name: the constant disc aspect ratio: the SPH artificial viscosity parameter α_{AV} : the binary eccentricity: the mass of the Be star: the mass of the neutron star and the mass of the SPH particles. The next three columns describe the Be star disc the end of the simulation: (left to right) the number of SPH particles in $R < a_b$ (when the binary is at apastron for the eccentric orbit binaries): the density weighted average smoothing length in the disc: the calculated value for the average viscosity parameter in the steady disc. The final three columns show the binary orbital period averaged flow rates of (left to right) the accretion rate onto the Be star: the accretion rate onto the neutron star and, finally, the rate of ejection of material.

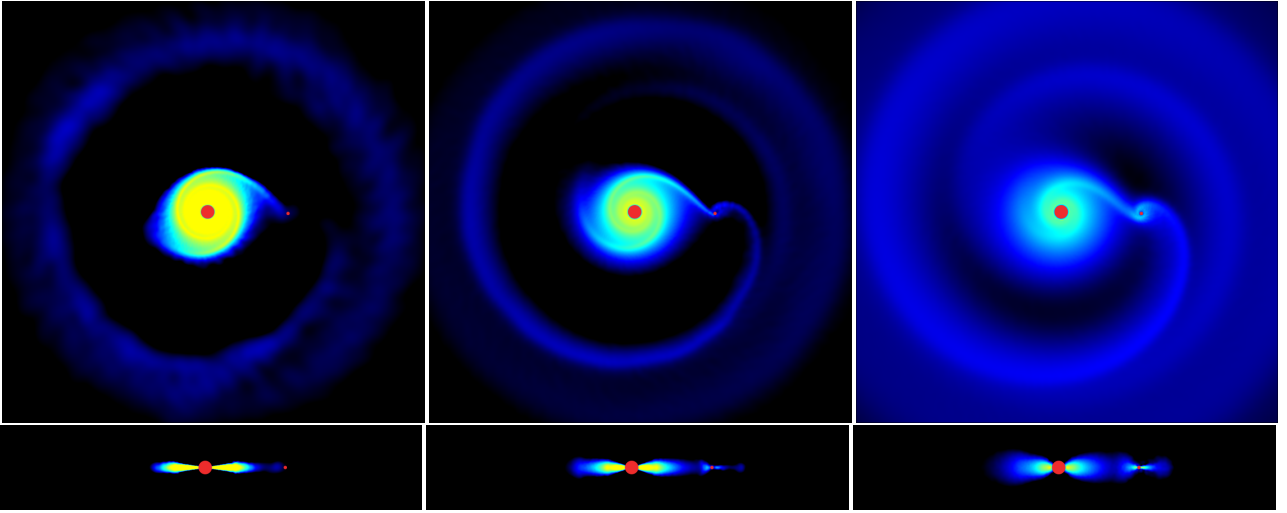


Figure 2. Visualizations of the steady state Be star disc for varying disc aspect ratio at a time of $t = 50 P_{\text{orb}}$. The Be star and neutron star are shown as red solid circles with the size scaled to their accretion radius. In each panel, the upper plot shows the $x - y$ plane in which the binary orbits while the lower panel shows a cross section of the disc in the $x - z$ plane. The disc aspect ratio is $H/R = 0.05$ (left, sim1), 0.1 (middle, sim2) and 0.2 (right, sim3). The panels have a size of $500 R_{\odot} \times 500 R_{\odot}$ (upper) and $500 R_{\odot} \times 100 R_{\odot}$ (lower).

that we can isolate its effects. The disc is locally isothermal with $T \propto R^{-1}$. The viscosity is implemented by modifying the SPH artificial viscosity. The values for α_{AV} are shown in Table 1 and $\beta_{AV} = 2$. The values for α_{AV} are chosen so that the Shakura & Sunyaev (1973) viscosity parameter, α , is close to either 0.1 or 0.01. This value is calculated with equation (38) in Lodato & Price (2010). It is not easy to obtain a predetermined value of α in the simulations because it depends upon the smoothing length $\langle h \rangle$ that changes with the surface density in the steady state disc. This requires iterating on values for α_{AV} in several simulations. Be stars are likely fully ionised and therefore have a relatively large viscosity, of the order of 0.1 (Jones et al. 2008; Carciofi et al. 2012; Ghoreyshi et al. 2018; Rímulo et al. 2018; Martin et al. 2019; Granada et al. 2021). We consider a lower value in addition for comparison.

The simulations are evolved for a time of $t = 50 P_{\text{orb}}$, where P_{orb} is the binary orbital period, except for sim4 that is evolved for $100 P_{\text{orb}}$. This is sufficient time for the Be star disc to reach a steady state. In the steady state, the number of particles in $R < a_b$, N_{steady} , averaged

over an orbital period is constant in time. Table 1 shows the input parameters of the simulations (the first 7 columns) and the properties of the steady state disc (next 3 columns). The smoothing length, $\langle h \rangle / H$, and the Shakura & Sunyaev (1973) viscosity α parameter are density weighted averages over the disc. The final three columns show the accretion rate onto the Be star, onto the neutron star and the ejection rate in the steady state averaged over an orbital period.

3.1 Effect of the disc aspect ratio

The first three simulations in Table 1 show the effect of increasing the disc aspect ratio. Fig. 1 shows the surface density profile for the Be star discs at the end of the simulations. The larger the disc aspect ratio the larger the size of the Be star disc. Fig. 2 shows the column density of the system viewed from face on and an edge on cross section for the same simulations. There is a transition in the size of the disc for $H/R \approx 0.1$. For smaller disc aspect ratio, the disc is effectively tidally truncated. However, for larger disc aspect ratio the

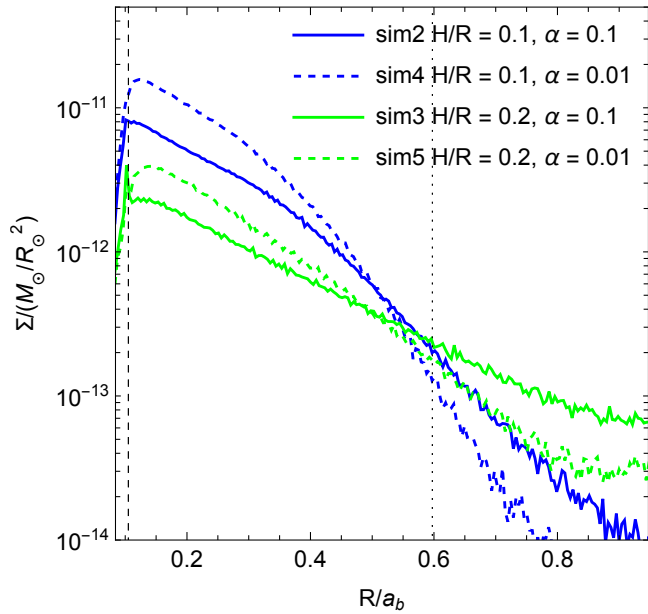


Figure 3. Same as Fig. 1 except the viscosity α parameter is varied in the dashed lines (sim4 and sim5). The solid lines are the same as in Fig. 1 (sim2 and sim3).

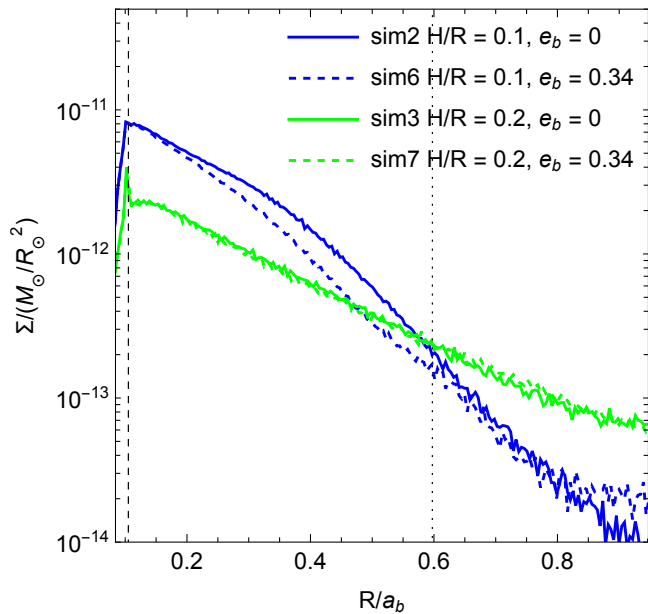


Figure 4. Same as Fig. 1 except the binary eccentricity is varied in the dashed lines (sim6 and sim7). The solid lines are the same as in Fig. 1 (sim2 and sim3). The surface density is shown while the binary is at apastron at time $t = 50 P_{\text{orb}}$.

tidal truncation becomes weaker. Disc material overflows the Roche lobe of the Be star and extends to the neutron star where a small disc forms around the neutron star (e.g. Hayasaki & Okazaki 2004, 2006). Material can also flow from the L2 point of the neutron star as a gas stream and this forms circumbinary material (e.g. Shu et al. 1979).

The final three columns in Table 1 show that for larger disc aspect ratio, less material is accreted onto the Be star and more material

flows outwards. The accretion rate onto the neutron star and the ejection rate both increase with disc aspect ratio. This is a result of a number of factors. First, a larger disc aspect ratio leads to a weaker tidal torque and a stronger viscous torque. This allows more material to flow outside of the Roche lobe of the Be star. Second, and a much smaller effect, is that the material is being added at Keplerian velocity while the velocity of the disc becomes more sub-Keplerian (see Section 3.7 in Martin et al. 2023). The ratio of the material accreted onto the neutron star compared to the material ejected decreases with increasing disc aspect ratio.

3.2 Effect of the viscosity parameter

We consider two simulations with a value for the α viscosity parameter that is smaller by a factor of 10, sim4 and sim5. Comparing these with sim2 and sim3 shows that if the value for α is decreased by a factor of 10, then the truncation efficiency, as defined by the accretion rate onto the star, is not significantly affected. Fig. 3 shows the steady state surface density profile in comparison to the larger α simulations. As expected, the simulations with a smaller α parameter have less material at larger radii since the truncation is a little more efficient. However, the relatively small change to the truncation efficiency for a large change to the viscosity parameter suggests that the truncation is more sensitive to the disc aspect ratio than the α parameter.

3.3 Effect of the binary eccentricity

We also consider some simulations with a non-zero binary eccentricity of $e_b = 0.34$ in sim6 ($H/R = 0.1$) and sim7 ($H/R = 0.2$). In general, the mild binary eccentricity does not significantly change the orbital period averaged accretion rates. The surface density profile for these is shown at apastron binary separation in Fig. 4 along with the circular orbit simulations for comparison. For the larger disc aspect ratio simulation ($H/R = 0.2$) that is not tidally truncated, there is little difference in the surface density profile with the increased eccentricity. There is also little change to the accretion rates onto the stars and the ejection rate. For the smaller disc aspect ratio simulation that is tidally truncated ($H/R = 0.1$), there is some difference in the surface density profile. This is because the tidal truncation radius of a disc scales with the binary eccentricity like $(1 - e_b)$ (Artymowicz & Lubow 1994; Hirsh et al. 2020). The smaller disc size leads to slightly larger outflow compared to accretion onto the Be star.

3.4 Effect of the binary mass ratio, $q = M_2/M_1$

Finally we consider a simulation with a smaller mass for the Be star, sim8, that has binary mass ratio of $q = M_2/M_1 = 0.14$. Comparing this with sim2 that has $q = 0.078$ shows that the larger mass ratio leads to a more efficient tidal truncation. In this case, there is no significant mass ejection from the binary. The accretion rate onto the neutron star is slightly lower compared with sim2.

4 CONCLUSIONS

We have performed hydrodynamic simulations of the formation of a steady state Be star accretion disc to examine its interaction with a companion neutron star. We consider the case that the Be star disc is coplanar to the binary orbital plane therefore maximising the tidal truncation efficiency. We have shown that the disc aspect ratio plays a crucial role in the truncation efficiency. The larger the disc aspect

ratio, the larger the rate of outflow through the disc and the larger the size of the disc. A disc with a small disc aspect ratio $H/R \lesssim 0.1$, is tidally truncated. The outflowing material is mostly accreted onto the neutron star through tidal streams. For larger disc aspect ratio, tidal truncation is weak and the disc fills the Roche lobe and extends out to the orbit of the neutron star. In this case, a large fraction of the outflowing material is ejected from the binary system. The effects of binary eccentricity are negligible on the disc structure for discs with large aspect ratio.

ACKNOWLEDGEMENTS

Computer support was provided by UNLV's National Supercomputing Center. RGM and SHL acknowledge support from NASA through grants 80NSSC21K0395 and 80NSSC19K0443. PJA and RGM acknowledge support from NASA TCAN award 80NSSC19K0639. We acknowledge the use of SPLASH (Price 2007) for the rendering of Fig. 2. The paper arose from our mutual interaction at the Kavli Institute for Theoretical Physics program on "Bridging the Gap: Accretion and Orbital Evolution in Stellar and Black Hole Binaries", funded by the National Science Foundation under Grant No. NSF PHY-1748958. SHL thanks the Simons Foundation for support of a visit to the Flatiron Institute.

DATA AVAILABILITY

The data underlying this article will be shared on reasonable request to the corresponding author.

REFERENCES

- Artymowicz P., Lubow S. H., 1994, *ApJ*, **421**, 651
- Bate M. R., Bonnell I. A., Clarke C. J., Lubow S. H., Ogilvie G. I., Pringle J. E., Tout C. A., 2000, *MNRAS*, **317**, 773
- Campana S., 1996, *Ap&SS*, **239**, 113
- Carciofi A. C., 2011, in Neiner C., Wade G., Meynet G., Peters G., eds, IAU Symposium Vol. 272, IAU Symposium. pp 325–336 ([arXiv:1009.3969](https://arxiv.org/abs/1009.3969)), doi:10.1017/S1743921311010738
- Carciofi A. C., Bjorkman J. E., 2006, *ApJ*, **639**, 1081
- Carciofi A. C., et al., 2006, *ApJ*, **652**, 1617
- Carciofi A. C., Okazaki A. T., Le Bouquin J. B., Štefl S., Rivinius T., Baade D., Bjorkman J. E., Hummel C. A., 2009, *A&A*, **504**, 915
- Carciofi A. C., Bjorkman J. E., Otero S. A., Okazaki A. T., Štefl S., Rivinius T., Baade D., Haubois X., 2012, *ApJ*, **744**, L15
- Coe M. J., Edge W. R. T., Galache J. L., McBride V. A., 2005, *MNRAS*, **356**, 502
- Cyr I. H., Jones C. E., Panoglou D., Carciofi A. C., Okazaki A. T., 2017, *MNRAS*, **471**, 596
- Eggleton P. P., 1983, *ApJ*, **268**, 368
- Franchini A., Martin R. G., 2019, *ApJ*, **881**, L32
- Franchini A., Lubow S. H., Martin R. G., 2019, *ApJ*, **880**, L18
- Fu W., Lubow S. H., Martin R. G., 2015, *ApJ*, **807**, 75
- Ghoreyshi M. R., et al., 2018, *MNRAS*,
- Granada A., Jones C. E., Sigut T. A. A., 2021, *ApJ*, **922**, 148
- Haberl F., Sturm R., 2016, *A&A*, **586**, A81
- Hanuschik R. W., 1996, *A&A*, **308**, 170
- Hayasaki K., Okazaki A. T., 2004, *MNRAS*, **350**, 971
- Hayasaki K., Okazaki A. T., 2006, *MNRAS*, **372**, 1140
- Heath R. M., Nixon C. J., 2020, *A&A*, **641**, A64
- Hirsh K., Price D. J., Gonzalez J.-F., Ubeira-Gabellini M. G., Ragusa E., 2020, *MNRAS*, **498**, 2936
- Jones C. E., Sigut T. A. A., Porter J. M., 2008, *MNRAS*, **386**, 1922
- Kozai Y., 1962, *AJ*, **67**, 591
- Lee U., Osaki Y., Saio H., 1991, *MNRAS*, **250**, 432
- Lidov M. L., 1962, *Planet. Space Sci.*, **9**, 719
- Liu Q. Z., van Paradijs J., van den Heuvel E. P. J., 2005, *A&A*, **442**, 1135
- Lodato G., Price D. J., 2010, *MNRAS*, **405**, 1212
- Lubow S. H., Ogilvie G. I., 2000, *ApJ*, **538**, 326
- Lubow S. H., Martin R. G., Nixon C., 2015, *ApJ*, **800**, 96
- Martin R. G., Lubow S. H., 2011, *MNRAS*, **413**, 1447
- Martin R. G., Nixon C., Armitage P. J., Lubow S. H., Price D. J., 2014a, *ApJL*, **790**, L34
- Martin R. G., Nixon C., Lubow S. H., Armitage P. J., Price D. J., Doğan S., King A., 2014b, *ApJL*, **792**, L33
- Martin R. G., Nixon C. J., Pringle J. E., Livio M., 2019, *New Astronomy*, **70**, 7
- Martin R. G., Armitage P. J., Lubow S. H., Price D. J., 2023, *ApJ*, **953**, 2
- Miranda R., Lai D., 2015, *MNRAS*, **452**, 2396
- Monaghan J. J., 1992, *ARA&A*, **30**, 543
- Moritani Y., et al., 2013, *PASJ*, **65**, 83
- Negueruela I., et al., 1997, *MNRAS*, **284**, 859
- Negueruela I., Reig P., Coe M. J., Fabregat J., 1998, *A&A*, **336**, 251
- Negueruela I., Okazaki A. T., Fabregat J., Coe M. J., Munari U., Tomov T., 2001, *A&A*, **369**, 117
- Nixon C. J., Pringle J. E., 2020, *ApJ*, **905**, L29
- Okazaki A. T., Negueruela I., 2001, *A&A*, **377**, 161
- Okazaki A. T., Bate M. R., Ogilvie G. I., Pringle J. E., 2002, *MNRAS*, **337**, 967
- Okazaki A. T., Hayasaki K., Moritani Y., 2013, *PASJ*, **65**, 41
- Panoglou D., Carciofi A. C., Vieira R. G., Cyr I. H., Jones C. E., Okazaki A. T., Rivinius T., 2016, *MNRAS*, **461**, 2616
- Papaloizou J., Pringle J. E., 1977, *MNRAS*, **181**, 441
- Papaloizou J. C. B., Terquem C., 1995, *MNRAS*, **274**, 987
- Porter J. M., 1996, *MNRAS*, **280**, L31
- Porter J. M., Rivinius T., 2003, *PASP*, **115**, 1153
- Price D. J., 2007, *Publ. Astron. Soc. Australia*, **24**, 159
- Price D. J., 2012, *Journal of Computational Physics*, **231**, 759
- Price D. J., Federrath C., 2010, *MNRAS*, **406**, 1659
- Price D. J., et al., 2018, *Publ. Astron. Soc. Australia*, **35**, e031
- Pringle J. E., 1991, *MNRAS*, **248**, 754
- Quirrenbach A., et al., 1997, *ApJ*, **479**, 477
- Reig P., 2011, *Ap&SS*, **332**, 1
- Rímulo L. R., et al., 2018, *MNRAS*, **476**, 3555
- Rivinius T., Carciofi A. C., Martayan C., 2013, *A&ARv*, **21**, 69
- Rubio A. C., et al., 2023, *MNRAS*, **526**, 3007
- Shakura N. I., Sunyaev R. A., 1973, *A&A*, **24**, 337
- Shu F. H., Lubow S. H., Anderson L., 1979, *ApJ*, **229**, 223
- Sigut T. A. A., McGill M. A., Jones C. E., 2009, *ApJ*, **699**, 1973
- Slettebak A., 1982, *ApJs*, **50**, 55
- Stella L., White N. E., Rosner R., 1986, *ApJ*, **308**, 669
- Suffak M., Jones C. E., Carciofi A. C., 2022, *MNRAS*, **509**, 931
- Suffak M. W., Jones C. E., Carciofi A. C., de Amorim T. H., 2023, *MNRAS*, **526**, 782
- Wood K., Bjorkman J. E., 1997, *ApJ*, **477**, 926
- von Zeipel H., 1910, *Astronomische Nachrichten*, **183**, 345

This paper has been typeset from a $\text{\TeX}/\text{\LaTeX}$ file prepared by the author.